Journal of Molecular Catalysis A: Chemical 325 (2010) 73–78

Contents lists available at ScienceDirect

Journal of Molecular Catalysis A: Chemical

journal homepage: www.elsevier.com/locate/molcata

ESR study of competition between Fe^{3+} and Cu^{2+} active sites for NO_x selective catalytic reduction by NH_3 in Cu–Fe-Beta catalyst

Alexei V. Kucherov[a,*], Dmitry E. Doronkin[a], Alexandr Yu. Stakheev[a], Arkady L. Kustov[b], Marie Grill[b]

[a] N.D. Zelinsky Institute of Organic Chemistry, Russian Academy of Sciences, 119991 Leninsky Prosp. 47, Moscow, Russia
[b] Haldor Topsøe A/S, P.O. Box 213, Nymøllevej 55, DK-2800 Lyngby, Denmark

ARTICLE INFO

Article history:
Received 16 February 2010
Received in revised form 25 March 2010
Accepted 26 March 2010
Available online 3 April 2010

Keywords:
Cu–Fe-Beta
NO_x-SCR
ESR

ABSTRACT

A series of Fe-Beta catalysts modified with different amount of Cu was prepared and tested in NO_x selective catalytic reduction by NH_3. ESR study reveals that replacement of isolated tetrahedral Fe^{3+} ions by Cu^{2+} ions in cationic sites of the zeolite takes place upon Fe-Beta treatment by copper. This modification results in gain in deNO_x activity in low-temperature region, due to formation of cationic Cu^{2+}, and significant loss in activity at high temperatures, which is determined by substitution of active Fe^{3+} for less active Cu^{2+}.

1. Introduction

Iron-containing zeolites (mostly Fe-ZSM-5 and Fe-Beta) are known to be effective catalysts for several applications including selective catalytic reduction (SCR) of NO_x by ammonia [1,2], N_2O decomposition and several other processes [3–5]. Most authors agree that active species of Fe-ZSM-5 and Fe-Beta catalysts in NH_3-deNO_x are isolated mononuclear Fe complexes located in the zeolite cationic positions [2,6–9]. These active sites have been characterized by various techniques including ESR, UV–vis, FTIR, Mössbauer spectroscopy and others [see e.g. 8]. Earlier we have noticed that active Fe^{3+} occupies only a fraction of Beta-zeolite cationic positions [7]. The non-occupied cationic positions can, in principle, host other metals providing new properties of the material. The examples of changing catalyst properties are the rise of hydrothermal stability in the case of Na [10] or decrease of overall activity of the catalyst as we observed in the case of Ca [7]. Cu-containing zeolites are known for their remarkable low-temperature activity in NH_3-deNO_x [11,12]. Hence it may be interesting to load free cationic positions in Fe-Beta with copper in order to combine Cu and Fe active sites in the catalyst to improve its activity in deNO_x. ESR spectroscopy can be used as informative and sensitive method for studying valence and coordination state of both copper [13–16] and iron species [2,6–8,17–19]. Unfortunately, other methods (UV–Vis, FTIR, Mössbauer spectroscopy) are not sensitive enough for study of low-loaded samples.

Previously, several groups have attempted to combine two transition metal cations in the zeolite in order to affect its catalytic properties. Teraoka et al. reported an increase in the activity of ion-exchanged Cu-ZSM-5 after modification with Fe for NO_x-SCR with ethane [20]. On the contrary, negative effect of Cu^{2+} on the methanol oxidation activity accompanied by a substantial increase in the catalyst selectivity towards products of partial oxidation was reported by Kustov et al. [21].

The aim of this paper is to investigate the behavior of Fe^{3+} active sites for NH_3-deNO_x in the presence of copper. Since high mobility of the cations in the zeolites can be obtained at high temperatures and in the presence of water [10] hydrothermal stability of the catalysts was additionally studied.

In order to investigate the effect of Cu on Fe-Beta several Cu–Fe-Beta catalysts have been prepared with varying the amount of Cu introduced into the parent Fe-Beta and tested in the reaction of SCR of NO_x by NH_3. The activity results obtained were interpreted based on ESR study of distribution of Fe^{3+} and Cu^{2+} paramagnetic species in the catalysts.

2. Experimental

2.1. Catalyst preparation

Parent 0.15 wt.% Fe-Beta was prepared by incipient wetness impregnation of commercial Beta (β) zeolite with a $Fe(NO_3)_3$ solution. The zeolite with SiO_2/Al_2O_3 ratio ≈ 25, H-form, was calcined at 550 °C in dry air flow for 4 h prior to Fe loading. The resulting material, designated as 0.15Fe-β, was dried overnight and divided into two portions. One portion was hydrothermally treated. The

* Corresponding author. Tel.: +7 495 137 6617; fax: +7 499 135 5328.
E-mail address: akuchero2004@yahoo.com (A.V. Kucherov).

1381-1169/$ – see front matter © 2010 Elsevier B.V. All rights reserved.
doi:10.1016/j.molcata.2010.03.035

Table 1
List of the studied catalysts and their treatment conditions.

#	Sample	Loaded Fe (wt.%)	Loaded Cu (wt.%)	Treatment conditions
1	β	–	–	HT
2	1.3Cu-β	–	1.3	Cu loading → HT
3	1.5Cu-β	–	1.5	Cu loading → HT
4	0.15Fe-β	0.15	–	Fe loading → HT
5	0.25Cu-HT-0.15Fe-β	0.15	0.25	Fe loading → HT → Cu loading → HT
6	0.75Cu-HT-0.15Fe-β	0.15	0.75	Fe loading → HT → Cu loading → HT
7	0.75Cu–0.15Fe-β	0.15	0.75	Fe loading → calcination → Cu loading → HT
8	1.0Cu-HT-0.15Fe-β	0.15	1.0	Fe loading → HT → Cu loading → HT
9	1.25Cu-HT-0.15Fe-β	0.15	1.25	Fe loading → HT → Cu loading → HT
10	1.5Cu-HT-0.15Fe-β	0.15	1.5	Fe loading → HT → Cu loading → HT
11	1.5Cu–0.15Fe-β	0.15	1.5	Fe loading → calcination → Cu loading → HT

conditions of hydrothermal treatment (HT) were as follows: calcination at 750 °C in air flow with 1.5% H_2O for 4 h. The other portion was calcined for 4 h at 550 °C in dry air.

Both portions of the 0.15Fe-β catalyst were then loaded with different amounts of copper (0.25–1.5 wt.% Cu) using incipient wetness impregnation with a solution of $Cu(NO_3)_2$. After that, samples were dried and hydrothermally treated. The list of prepared catalysts, with preparation stages, is given in Table 1.

2.2. Catalysis

The catalytic measurements were carried out in a fixed-bed quartz flow reactor (inner diameter = 8 mm) while temperature was decreased from 550 to 150 °C with a rate 3 °C/min. Catalyst (0.12 g, d = 0.4–1 mm) was diluted with 0.5 ml of ~1 mm granules of γ-Al_2O_3 (LaRoche) and placed on a quartz wool bed. Prior to these experiments, the catalytic activity of γ-Al_2O_3 was measured and confirmed to be zero throughout the temperature region of 100–550 °C. The gas composition was: 7.5% O_2, 10% CO_2, 4% water, 310 ppm NH_3 and 300 ppm NO balanced with N_2, GHSV = 150 000 h^{-1}. Reaction products were analyzed by an Eco Physics CLD 822 chemiluminescent NO_x analyzer.

Catalytic activity was calculated based on NO_x conversion as a first-order rate constant ($cm^3/g/s$) using the following equation:

$$k = -\frac{F_{NO}}{m_{cat} \cdot C_{NO}} \cdot \ln(1 - X)$$

where F_{NO} denotes the molar feed rate of NO (mol/s), m_{cat} is the catalyst weight, C_{NO} is the NO concentration (mol/cm^3), and X is the fractional conversion of NO_x. Throughout the whole temperature range studied considerable part of NH_3 remained unconverted (Table 2). Therefore, competitive oxidation of ammonia by O_2 can be not accounted when calculating catalysts activity.

2.3. Electron paramagnetic resonance

The ESR signals from both Cu^{2+} and Fe^{3+} ions were recorded in the X-band ($\lambda \cong 3.2$ cm) at 20 and −196 °C on a spectrometer equipped with a 4104OR cavity and a co-axial quartz Dewar. The ESR signals were registered in the lack of saturation in the field range of 0–3900 G. Samples were studied after catalytic testing.

The crushed samples (0.4–1.0 mm) of equal weight (0.12 g) were placed in identical glass ampoules (d = 2.5 mm), connected to the vacuum system, evacuated at 90 °C for 2–3 min to 0.03 Torr, and sealed off. Then the ESR spectra were registered at 20 and −196 °C. After that samples in ampoules were impregnated with pyridine (chemically pure grade), kept 1 h at room temperature, and the ESR spectra were registered at −196 °C for quantitative determination of isolated Fe^{3+} cations according to procedure described in [17]. For highest accuracy, sets of samples were measured consecutively, with ampoules in the same position inside the ESR resonator. No absolute standard was used for calibration: all ESR intensity data were calculated by normalized double integration and presented in arbitrary units which is sufficient for our purpose—to monitor relative variations of concentration of both Cu^{2+} and Fe^{3+} species.

3. Results

3.1. Catalytic data

NO_x and NH_3 conversions over studied catalysts are given in Table 2. NH_3 adsorption on zeolite impedes precise measurement of NH_3 concentration at low-temperature. Thus, the data on NH_3 conversion may be used for rough estimation. Still from the analysis of NH_3 conversions in Table 2 one may conclude that throughout the whole temperature range studied considerable part of NH_3 remains unconverted. In general, NH_3 conversion followed the same trend

Table 2
Performance of studied catalysts in NH_3-deNO_x.

#	Sample	Conversion @ 175 °C, %		Conversion @ 385 °C, %	
		NO_x	NH_3	NO_x	NH_3
1	β	0.0	4.4	37.3	44.5
2	1.3Cu-β	9.2	23.8	31.6	39.7
3	1.5Cu-β	12.3	32.4	36.8	48.8
4	0.15Fe-β	0.3	9.5	66.5	78.5
5	0.25Cu-HT-0.15Fe-β	1.9	7.3	62.1	66.3
6	0.75Cu-HT-0.15Fe-β	2.1	13.1	40.6	39.3
7	0.75Cu–0.15Fe-β	2.8	12.7	56.8	52.0
8	1.0Cu-HT-0.15Fe-β	5.8	13.3	34.4	35.8
9	1.25Cu-HT-0.15Fe-β	9.2	10.1	32.9	33.9
10	1.5Cu-HT-0.15Fe-β	11.3	14.8	34.6	42.8
11	1.5Cu–0.15Fe-β	17.9	27.0	58.1	59.9

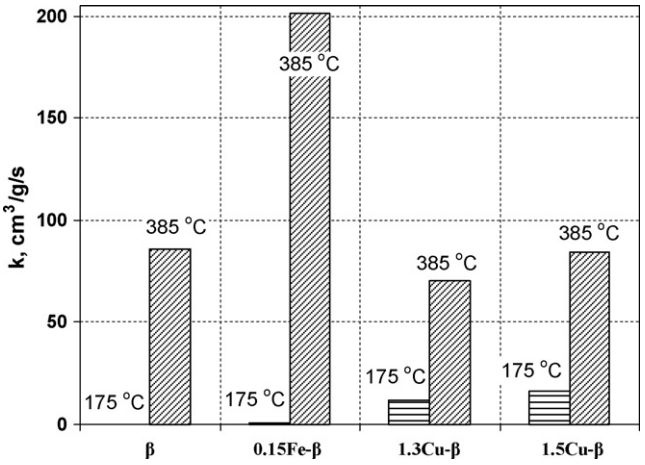

Fig. 1. First-order rate constant of the NH_3-deNO_x process (cm^3 NO_x/g/s) for parent β, β loaded with 0.15 wt.% Fe, and 1.3–1.5 wt.% Cu. Reaction conditions: 7.5% O_2, 10% CO_2, 4% H_2O, 300 ppm NH_3 and 300 ppm NO balanced with N_2, GHSV = 150 000 h^{-1}.

as NO_x conversion, so we used the latter to calculate catalyst activity.

Using values of NO_x conversion the activity of the catalysts was calculated as a first-order rate constant. Parent β zeolite (hydrothermally treated) shows some activity in the temperature range 270–550 °C (see data at 385 °C in Fig. 1). Taking into account our previous results [7] we attribute this intrinsic activity of the parent zeolite to the contaminating traces of iron, which is 270 ppm according to ICP-OES. Loading of additional 0.15 wt.% Fe causes a considerable rise in deNO_x activity of the catalyst in the temperature range 200–550 °C (Fig. 1).

Loading of the parent β zeolite with 1.3 or 1.5 wt.% of Cu results in considerable increase in activity of the catalyst in the low-temperature region (100–250 °C, see data at 175 °C in Fig. 1). At the same time, the deNO_x activity of 1.3 or 1.5Cu-β in the high-temperature region does not exceed that of parent β zeolite. Thus, copper introduction seems to result in a gain in catalytic activity only at low temperatures.

The activity data for Cu-containing 0.15Fe-β catalysts with Cu concentrations ranging from 0.25 to 1.5 wt.% is presented in Fig. 2. It can be seen that loading of 0.25 wt.% of Cu slightly decreases the activity of 0.15Fe-β at 385 °C while at 175 °C NO_x conversion increases. Loading of 0.75 wt.% of Cu results in a drastic suppression of the deNO_x activity of 0.15Fe-β catalysts at 385 °C. Increase in Cu concentration up to 1.0 wt.% results in further decrease of the catalyst activity at 385 °C accompanied by an increase in NO_x conversion at 175 °C. Finally, loading of 1.5 wt.% Cu results in activity increase at both temperatures (175 and 385 °C).

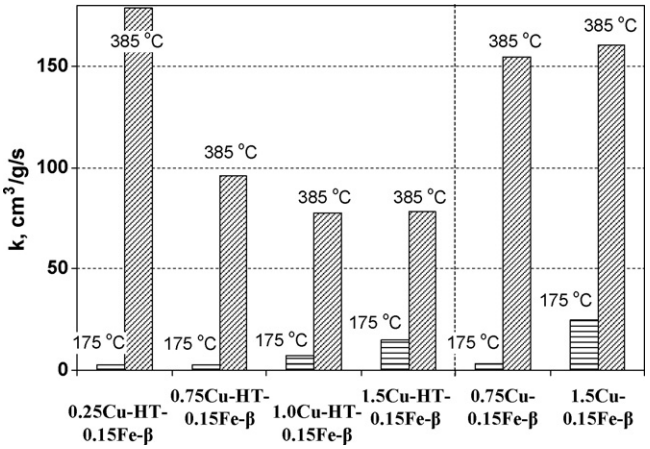

Fig. 2. Influence of loading of 0.25–1.5 wt.% Cu on the deNO_x first-order rate constant for hydrothermally pretreated and just calcined 0.15Fe-β catalyst. Reaction conditions: 7.5% O_2, 10% CO_2, 4% H_2O, 300 ppm NH_3 and 300 ppm NO balanced with N_2, GHSV = 150 000 h^{-1}.

To estimate the effect of hydrothermal treatment of Fe-Beta before Cu loading, two samples, 0.75Cu–0.15Fe-β and 1.5Cu–0.15Fe-β, were prepared in a different way. After loading with Fe these samples were calcined in dry air at 550 °C instead of being hydrothermally treated. After introducing 0.75 and 1.5 wt.% Cu these bimetallic catalysts, were hydrothermally treated at 750 °C (conditions identical for all catalysts in this work). The catalytic data for these catalysts are presented in Fig. 2 along with catalysts prepared in traditional way (double hydrothermal treatment after Fe loading and after Cu loading). From the comparison of activity of 0.75Cu–0.15Fe-β with that of 0.75Cu-HT-0.15Fe-β it is evident that hydrothermal treatment after Fe loading suppresses high-temperature activity of Fe^{3+} severely but low-temperature activity caused by copper addition remains essentially unchanged. For the pair of samples with higher Cu loading, with and without repeated HT treatment (1.5Cu–0.15Fe-β and 1.5Cu-HT-0.15Fe-β), additional hydrothermal treatment results in decrease of both low-temperature activity ascribed to Cu and high-temperature activity determined by Fe.

3.2. Electron paramagnetic resonance

ESR spectra of evacuated samples can be characterized by two signals: (1) a rather weak narrow low-field line at $g = 4.27$ (ascribed to isolated tetrahedrally coordinated Fe^{3+} species in zeolites [2,6–8,17]) and (2) a complex signal at $g_{||} = 2.35–2.38$, $g_{\perp} = 2.06–2.07$ being typical of isolated Cu^{2+} ions in different coordinations [13–16]. The superimposed very broad signal at $g \approx 2.0$ which is characteristic for interacting octahedral Fe^{3+} ions (residual Fe_2O_3 phase) is negligibly small.

The intensity of the Fe^{3+}-ESR signal at $g = 4.27$ increases substantially at temperature of liquid nitrogen due to the Curie–Weiss law, but unfortunately the noise level rises at the same time. Impregnation of the samples with pyridine causes both narrowing of the Fe^{3+}-ESR signal at $g = 4.27$ and intensity rise by a factor of ~1.5. It indicates that pyridine filling zeolitic channels affects the relaxation conditions of the tetrahedral paramagnetic Fe^{3+} sites. Similar effect of pyridine bonding with isolated Fe^{3+} sites was demonstrated earlier in H-ZSM-5 [17]. The effect observed is illustrated in Fig. 3a. This approach allows to improve sensitivity and accuracy of Fe^{3+} ESR measurements. Thus, in this study all Fe^{3+} signals from the samples are recorded at −196 °C after pyridine impregnation, and the results are summarized in Fig. 3.

The Cu^{2+} region of the ESR spectra is shown in Fig. 4 where signals from evacuated 0.75Cu-HT-0.15Fe-β sample and the same sample impregnated with pyridine are given. Signals from the two samples are practically identical in shape and differ only in intensity. ESR spectra for evacuated samples contain signals at $g_{||} \sim 2.38$, $A \sim 120$ G, and $g_{\perp} \sim 2.07$ (Fig. 4a), which is typical for octahedrally coordinated isolated Cu^{2+} ions. This coordination is common for zeolitic samples containing adsorbed water (which cannot be removed by a short-term evacuation). Filling of zeolitic channels with pyridine molecules causes rearrangement of copper(II)-sites by these strong and bulky ligands, and the resulting ESR signal corresponds to five-coordinated isolated Cu^{2+} sites ($g_{||} \sim 2.35$, $A \sim 156$ G, and $g_{\perp} \sim 2.06$) (Fig. 4b). From a practical point of view, signals are quite intense even for samples evacuated at 20 °C, so relative changes in concentration of zeolitic Cu^{2+}-sites *vs.* the amount of copper added can be evaluated from these data, as shown in Fig. 5.

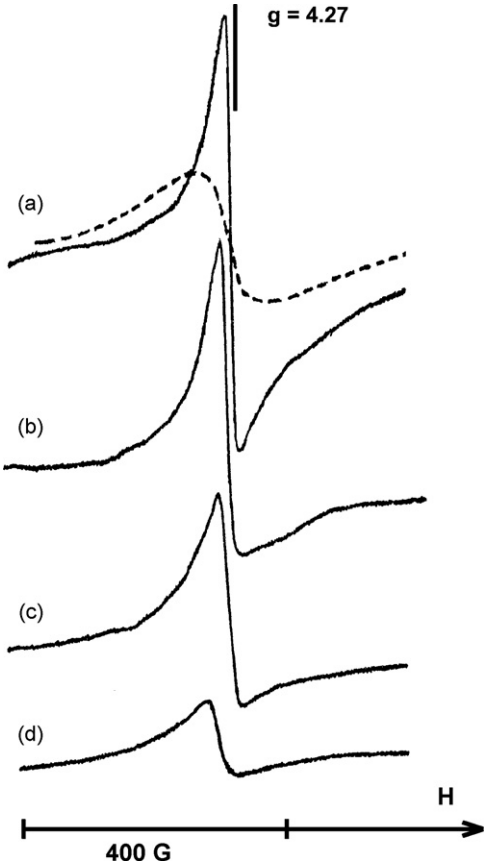

Fig. 3. Changes of the ESR signal from isolated tetrahedral Fe^{3+} sites ($g = 4.27$) caused by increasing Cu loading in Cu-HT-0.15Fe-β catalysts: (a) no Cu; (b) 0.25 wt.%, Cu; (c) 0.75 wt.%, Cu; (d) 1.5 wt.%, Cu. Recorded at −196 °C after impregnation with pyridine; dotted line: recorded at 20 °C after evacuation.

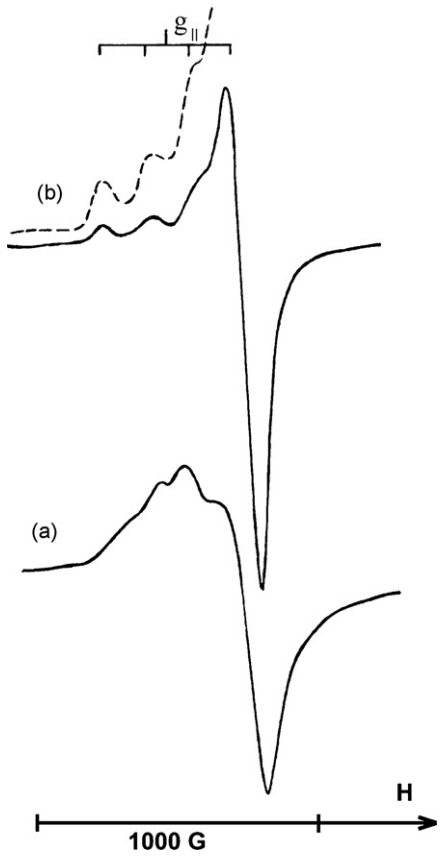

Fig. 4. ESR signal from isolated Cu^{2+} species in 0.75Cu-HT-0.15Fe-β: (a) at 20 °C under vacuum; (b) at −196 °C after impregnation with pyridine.

4. Discussion

It is important to note that in our ESR study of pyridine adsorption, the effect caused by this ligand is clearly seen for both Fe^{3+} ions (Fig. 3a) and Cu^{2+} ions (Fig. 4). This fact confirms the non-rigid, cationic arrangement of both paramagnetic species under consideration.

The dependence of the number of isolated tetrahedral Fe^{3+} sites from the amount of copper introduced is shown in Fig. 6. Increase in the amount of copper added to Fe-β is accompanied by a gradual decrease in concentration of ESR-visible Fe^{3+} sites by a factor of ~10 (Fig. 6a). Plotting of the data *vs.* concentration of ESR-visible paramagnetic Cu^{2+} cations (Fig. 6b) seems to be even more indicative: increase in the amount of Cu^{2+} sites causes a linear drop of the amount of Fe^{3+} sites down to a small residual value. The amount of copper which is necessary for nearly complete disappearance of ESR-visible Fe^{3+} sites does not exceed ~1 wt.%. Even an addition of 0.25 wt.%. Cu causes a measurable loss of the number of isolated tetrahedral Fe^{3+} sites (Fig. 6). It indicates that Cu^{2+} cations replace Fe^{3+} in zeolitic cationic positions quite efficiently instead of occupying free cationic positions as was expected initially.

The first feature observed during the activity measurements is an appearance and gradual rise of activity at 175 °C for the samples with increasing Cu content. It should be noted that both starting β and 0.15%Fe-β demonstrate zero activity at such low temperature (Fig. 1). Therefore it is interesting to correlate an observed increase in the catalyst activity with the amount of Cu^{2+} paramagnetic sites formed (Fig. 5). Fig. 7 shows the dependence of the rate constant at 175 °C on the intensity of the ESR signal of Cu^{2+} ions (in arbitrary units). Good linear correlation between the activity and the content of ESR-visible Cu^{2+} in the catalysts (Fig. 7) can be observed. This fact indicates that formation of Cu^{2+} cations in the starting inactive Fe-β is responsible for the activity of the catalyst at low temperature.

The situation is quite opposite for high-temperature catalyst activity. Starting 0.15Fe-β demonstrates a very high catalytic activity at 385 °C (Fig. 1), and the catalyst activity under these conditions is determined by Fe^{3+} active sites. Introduction of copper causes a very pronounced drop in high-temperature activity of bimetallic

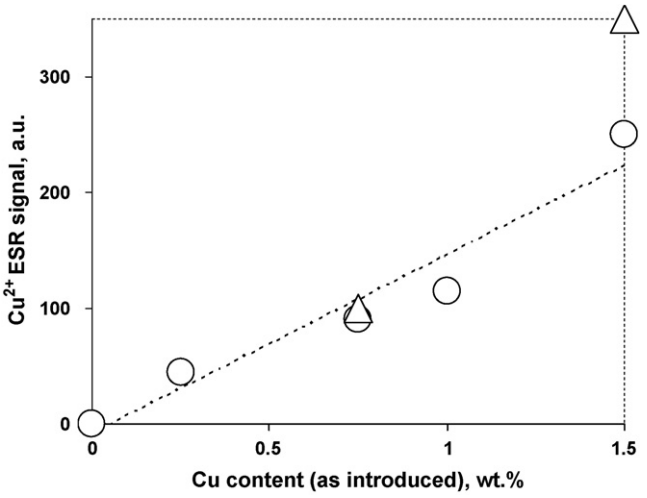

Fig. 5. Increase of concentration of ESR-visible Cu^{2+} species in Cu–Fe-β catalysts caused by increasing copper content. Recorded at 20 °C after evacuation. Rhomb marks stand for Cu-HT-0.15Fe-β, triangles for Cu–0.15Fe-β.

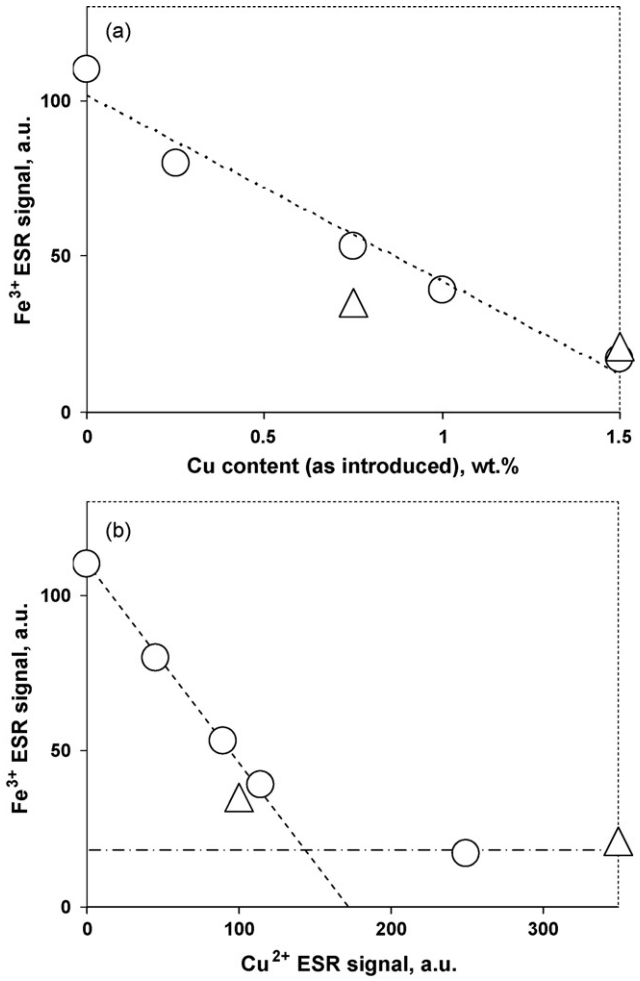

Fig. 6. Decrease of concentration of paramagnetic Fe^{3+} sites in Cu–Fe-β catalysts caused by increasing copper content: (a) *vs.* wt.% of copper added; (b) *vs.* concentration of ESR-visible Cu^{2+} paramagnetic sites. Round marks stand for Cu-HT-0.15Fe-β, triangles for Cu–0.15Fe-β.

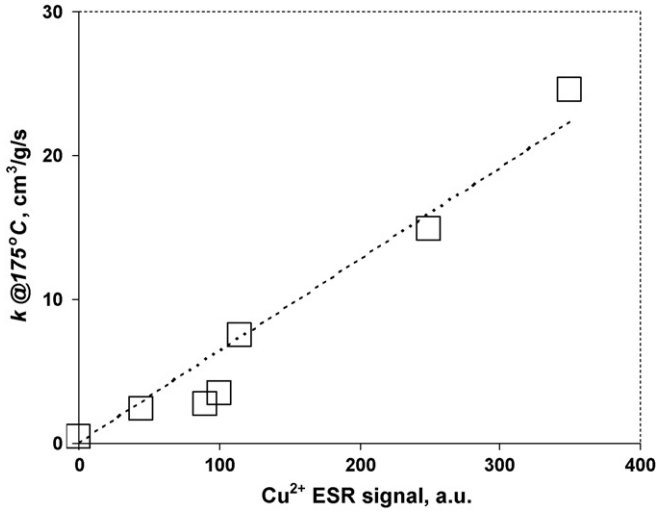

Fig. 7. Dependence of the NH_3-deNO_x first-order rate constant (cm^3 NO_x/g/s) measured at 175 °C on the intensity of ESR signal of Cu^{2+} for Cu–Fe-β catalysts. .

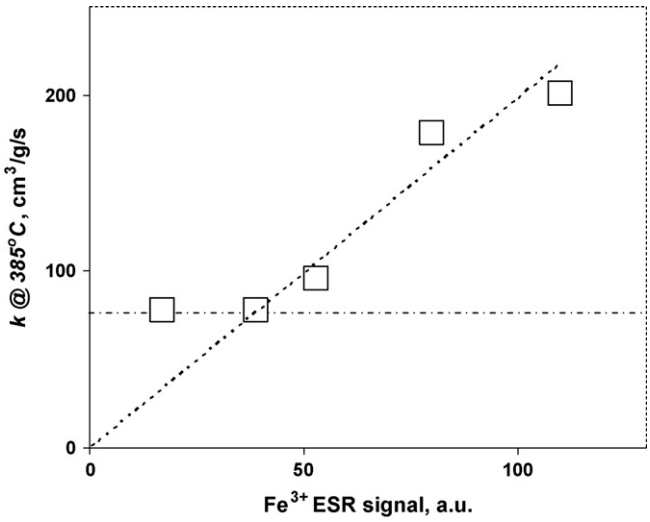

Fig. 8. Dependence of the NH_3-deNO_x first-order rate constant (cm^3 NO_x/g/s) measured at 385 °C on the intensity of ESR signal of Fe^{3+} for Cu-HT-Fe-β catalysts. Dash and dotted line stands for the activity of 1.5Cu-β.

samples. The first-order rate constant at 385 °C decreases linearly with decrease in the concentration of Fe^{3+} cations represented by an ESR signal at $g = 4.27$ (Fig. 8). This decrease in the number of Fe^{3+}-sites is evidently caused by loading of Cu into the catalyst. Since new formed Cu^{2+}-sites are also active in NH_3-deNO_x, the rate constant measured at 385 °C does not drop to zero. With a decrease in concentration of active Fe^{3+} species the rate constant reaches a lower level characteristic for Cu-β (Fig. 8). Iron seems to have no remaining effect on the catalytic activity of bimetallic samples with Cu content exceeding 1.25 wt.%. Further increase in Cu loading (to 1.5 wt.%) leads to increase in the concentration of active Cu^{2+} and consequent increase in the catalyst activity at both low and high temperatures.

Thus, introduction of Cu into Fe-β catalysts results in the replacement of a main part of Fe^{3+} in the active positions which is followed by the lowering of SCR activity at high temperature and some gain in activity at low temperatures.

Analysis of the results for Cu–Fe-β samples pretreated in a different way (hydrothermally treated at 750 °C *vs.* calcined at 500 °C) demonstrates that both concentration of ESR-visible Cu^{2+} sites (Fig. 5) and catalytic activity of the 1.5Cu–0.15Fe-β (Fig. 2) are substantially higher than for the Cu-HT-0.15Fe-β. In other words, copper introduction into the sample calcined under mild conditions results in stabilization of a larger fraction of Cu^{2+} cations by the zeolite. As a result, this data plotted in Fig. 7 fits overall linear dependence. This effect can be explained if we assume that hydrothermal treatment of 0.15Fe-β prior to Cu loading leads to partial destruction of framework Al-sites. Thus, HT results in loss of zeolite acid sites able to host metal cations. This could easily happen since only ~5% of all cationic positions are occupied by Fe, leaving a major part of protonic cationic positions free of Fe^{3+}. In the case of 1.5Cu–0.15Fe-β sample, more cationic positions are remaining to host Cu^{2+} after mild calcination of the parent material and the Cu^{2+}-sites formed are more stable against final hydrothermal treatment of bimetallic sample. Similar stabilizing effect of Cu^{2+} was demonstrated earlier for H-ZSM-5 samples [22]. Thus, the introduction of Cu^{2+} before hydrothermal treatment seems to provide a better protection of the cationic sites from destruction.

Then analyzing activity of the samples pretreated in a different way it should be noted that, in principle, acid sites might influence NH_3-deNO_x over zeolites. However in [6] we demonstrated that the rate of NH_3-deNO_x over Fe-Beta zeolites with number of

acid sites differing by an order of magnitude depend only on concentration of redox Fe^{3+} sites, as seen by ESR. In [7] we also noted that different acidity of Fe-[H]Beta and Fe-[Ca]Beta did not influence intrinsic activity of Fe^{3+}. Thus active sites Fe^{3+} have the same turnover number (reaction rate per active Fe) for zeolites with different acidity. That is why we do not consider change in zeolite acidity after HT to be the main factor causing decrease of the catalysts high-temperature activity.

5. Conclusions

By combining activity measurements and ESR investigation it was shown that modification of Fe-Beta catalysts with copper results in a decrease in concentration of active Fe^{3+} species because of their replacement in zeolite cationic positions by Cu^{2+}. Therefore, this modification results in gain in deNO_x activity in low-temperature region (determined by Cu^{2+} only) together with significant loss in activity in high-temperature region (determined by substitution of active Fe^{3+} for less active Cu^{2+}).

Acknowledgments

The authors wish to thank Haldor Topsøe A/S for financial support of this work. D. Doronkin is also grateful to Haldor Topsøe A/S for financial support in the framework of Ph.D. student support programme.

References

[1] H. Huang, R.Q. Long, R.T. Yang, Applied Catalysis A: General 235 (2002) 241–251.
[2] M.S. Kumar, M. Schwidder, W. Grünert, A. Brückner, Journal of Catalysis 227 (2004) 384–397.
[3] K.A. Dubkov, N.S. Ovanesyan, A.A. Shteinman, E.V. Starokon, G.I. Panov, Journal of Catalysis 207 (2002) 341–352.
[4] L.V. Pirutko, V.S. Chernyavsky, E.V. Starokon, A.A. Ivanov, A.S. Kharitonov, G.I. Panov, Applied Catalysis B: Environmental 91 (2009) 174–179.
[5] I. Yuranov, D.A. Bulushev, A. Renken, L. Kiwi-Minsker, Applied Catalysis A: General 319 (2007) 128–136.
[6] D.E. Doronkin, A.Yu. Stakheev, A.V. Kucherov, N.N. Tolkachev, G.O. Bragina, G.N. Baeva, P. Gabrielsson, I. Gekas, S. Dahl, Mendeleev Communications 17 (2007) 309–310.
[7] D. Doronkin, A. Stakheev, A. Kucherov, N. Tolkachev, M. Kustova, M. Høj, G. Baeva, G. Bragina, P. Gabrielsson, I. Gekas, S. Dahl, Topics in Catalysis 52 (2009) 1728–1733.
[8] M. Santhosh Kumar, M. Schwidder, W. Grunert, U. Bentrup, A. Bruckner, Journal of Catalysis 239 (2006) 173–186.
[9] G. Qi, R.T. Yang, Applied Catalysis B: Environmental 60 (2005) 13–22.
[10] J.A.Z. Pieterse, G.D. Pirngruber, J.A. van Bokhoven, S. Booneveld, Applied Catalysis B: Environmental 71 (2007) 16–22.
[11] T. Komatsu, M. Nunokawa, I.S. Moon, T. Takahara, S. Namba, T. Yashima, Journal of Catalysis 148 (1994) 427–437.
[12] J.A. Sullivan, J. Cunningham, M.A. Morris, K. Keneavey, Applied Catalysis B: Environmental 7 (1995) 137–151.
[13] A.V. Kucherov, J.L. Gerlock, H.-W. Jen, M. Shelef, Catalysis Today 27 (1996) 79–84.
[14] A.V. Kucherov, H.G. Karge, R. Schlogl, Microporous and Mesoporous Materials 25 (1998) 7–14.
[15] A.V. Kucherov, A.N. Shigapov, A.A. Ivanov, M. Shelef, Journal of Catalysis 186 (1999) 334–344.
[16] J. Dědeček, Z. Sobalík, Z. Tvarůžková, D. Kaucký, B. Wichterlová, Journal of Physical Chemistry 99 (1995) 16327–16337.
[17] A.V. Kucherov, M. Shelef, Journal of Catalysis 195 (2000) 106–112.
[18] A.V. Kucherov, A.A. Slinkin, Journal of Physical Chemistry 93 (1989) 864–867.
[19] A.V. Kucherov, C.N. Montreuil, T.N. Kucherova, M. Shelef, Catalysis Letters 56 (1998) 173–181.
[20] Y. Teraoka, H. Ogawa, H. Furukawa, S. Kagawa, Catalysis Letters 12 (1992) 361–366.
[21] A.L. Kustov, E.E. Knyazeva, E.A. Zhilinskaya, A. Aboukais, B.V. Romanovsky, Studies in Surface Science and Catalysis 135 (2001) 350.
[22] A.V. Kucherov, C.P. Hubbard, M. Shelef, Journal of Catalysis 157 (1995) 603–610.